



## Enhanced adsorptive removal of cationic dyes from aqueous solution by chemically treated carob shells

M. Farnane<sup>a</sup>, A. Elhalil<sup>a</sup>, A. Machrouhi<sup>a</sup>, F.Z. Mahjoubi<sup>a</sup>, M. Sadiq<sup>a</sup>, M. Abdennouri<sup>a</sup>, S. Qourzal<sup>b</sup>, H. Tounsadi<sup>a,c,\*</sup>, N. Barka<sup>a</sup>

<sup>a</sup>Laboratoire des Sciences des Matériaux, des Milieux et de la Modélisation (LS3M), FPK, Univ Hassan 1, B.P. : 145, 25000 Khouribga, Morocco

<sup>b</sup>Equipe de Catalyse et Environnement, Département de Chimie, Faculté des Sciences, Université Ibn Zohr, B.P.8106 Cité Dakhla, Agadir, Morocco

<sup>c</sup>Université Sidi Mohamed Ben Abdellah, Faculté des Sciences Dhar El Mahraz, Fès, Morocco, Tel. +212 645 20 85 64, Fax +212 523 49 03 54, email: hananetounsadi@gmail.com (H. Tounsadi)

Received 14 July 2017; Accepted 19 November 2017

### ABSTRACT

The aim of this work was to study the removal of methylene blue (MB) and malachite green (MG) from aqueous solution by raw and chemically treated carob shells as low cost biosorbent. Samples were characterized by Boehm titration, elemental analysis (CHNOS), Fourier transform infrared spectroscopy (FT-IR), scanning electron microscopy (SEM) and the point of zero charge ( $pH_{pzc}$ ). The experimental results show that the biosorption yield increases with an increase in the biosorbent dosage. Maximum biosorption capacity occurred at basic pH medium. Kinetic data were analyzed using pseudo-first and pseudo-second kinetic models. Equilibrium data fit Langmuir model with maximum monolayer biosorption capacities of 217.15, 232.44 and 342.21 mg/g for MB and 233.40, 291.74 and 327.89 mg/g in the case of MG, respectively, for Raw-carb, HCl-carb and NaOH-carb. The temperature doesn't have much influence on the biosorption performance. The NaOH treated carob shells was considered to be strongly efficient for the removal of MB and MG from aqueous solutions.

*Keywords:* Carob shell; Chemical activation; Dyes removal; Kinetics; Equilibrium; Biosorption

### 1. Introduction

Dyes pollution of aqueous solutions poses serious problems for the environment and human beings [1]. Effluents charged with dyes may be due to various industries, such as paper, plastic, textile, cosmetics and leather. Most of dyes have complex aromatic molecular structure and are generally resistant to light, temperature and oxidizers [2]. This characteristic feature makes most of dyes non-degradable and therefore causes bio accumulation in living organisms, leading to severe diseases and disorders. Therefore, dyes itself are so toxic to some organism. Currently, due to their toxicity and their great potential environmental impact,

much attention has been focused for treating wastewater containing synthetic dyes [3,4].

Methylene blue is a cationic dye having various applications in chemistry, biology, medical science and dyeing industries. Its long-term exposure can cause vomiting, nausea, anemia and hypertension [5]. Then, another dye can be marked is malachite green. It is a triphenylmethane dye that is used extensively in many industrial and aquacultural processes, generating environmental concerns and health problems to human being [6,7].

Several methods have been used for dyes removal from wastewaters in order to decrease their impact on the environment. These methods include integrated chemical-biological degradation [8], photo degradation [9], coagulation [10], membrane filtration [11], and electrochemical methods [12]. Whereas, these techniques had a large of advantages and disadvantages. For example, the

\*Corresponding author.

biological methods take much time and cannot degrade complicated dyes [13]. Common chemical oxidation like using chlorine is firstly slow and needs reactive materials which are dangerous to transport and store [14]. Secondly, these methods are not efficient enough because there are various materials in wastewater. Advanced oxidation methods such as ozonation, photo catalysis, and photo fenton are costly and uneconomical [15]. Coagulation causes a production of selectivity sludge against pollutants, membrane filtration has Good ability to remove dyes and metal cations but it has a production of concentrated sludge, electrochemical methods where no chemical product required can be designed to withstand suspended solids. However, they are most costly. Therefore, there is a need for more effective and cheaper ways of treating textile wastewater which consume the smallest amounts of chemicals and energy.

Research into wastewater treatment has focused on adsorption over the past few years [16–20]. However, adsorption [21,22] is considered as a superior technique comparatively with other traditional treatment methods due to its simplicity of design, high efficiency, ease of operation and ability to treat dyes in a more concentrated form [23].

The most commonly used adsorbent is activated carbon, but its application is often limited due to its high cost. Besides the activated carbon, there are a variety of natural and low cost materials that can be considered as biosorbents comprising sugar extracted rice [24], olives stone [25], cotton stalk [26], Ziziphus lotus fruit peels and avocado kernels seeds [27], maize waste [28], mango seed [29], peanut husk [30], Opuntia ficus-indica fruit waste [31], teak leaf [32] and waste materials [33], bottom ash and de-oiled soya [34], wild carrot flower [35], Harra and Coronaria L. [36] for the removal of various dyes. In addition to these biosorbents, there is used as an efficient new biosorbent. It's a material very abundant and readily available; which its use to the wastewater treatment is not yet well recognized.

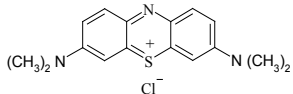
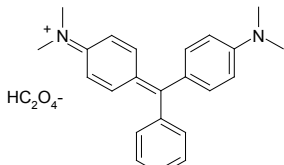
The aim of this study was to investigate the applicability of a chemically treated carob shell as a sorbent for the removal of methylene blue (MB) and malachite green (MG) from aqueous solution. Biosorption studies were carried out under various parameters such as solution pH, biosorbent dosage, contact time, initial dyes concentration and temperature. The biosorption kinetic data were tested by pseudo-first-order and pseudo-second-order kinetic models. The equilibrium data were analyzed using Langmuir, Freundlich, Temkin and Dubinin–Radushkevich isotherm models.

## 2. Materials and methods

### 2.1. Materials

All the necessary chemicals used in this study were of analytical grade. Methylene blue MB (85%) was purchased from Panreac (Spain). Malachite green MG (100%), NaCl (99.5%), HCl (37%), Na<sub>2</sub>CO<sub>3</sub> and NaHCO<sub>3</sub> were obtained from Sigma-Aldrich (Germany). HNO<sub>3</sub> (65%) from Scharlau (Spain) and NaOH (98%) was provided from Merck (Germany). The chemical structures and physical properties of MB and MG are shown in Table 1.

Table 1  
Physicochemical characteristics of used dyes

Name	Molecular structure	$M_w$ (g/mol)	$\lambda_{max}$ (nm)
Methylene blue (Basic blue 9)		319.85	661
Malachite green (Basic green 4)		329.5	621

### 2.2. Preparation of the biosorbents

The carob shell was gathered from the region of Khenifra in Morocco. Foremost, it was washed several times with distilled water to remove impurities and then dried at 70°C for 24 h, crushed and sieved to the desired particle sizes <160 µm referred as Raw-carb.

Into the chemical pretreatments, 10 g the Raw-carb treated with 100 mL of 1 M solution of HCl or NaOH for 2 h. The biosorbents were then filtered and washed with distilled water until neutral pH. The pretreated biosorbents were then dried in an oven at 80°C for 24 h and stored in glass bottles under to following names HCl-carb and NaOH-carb for later use.

### 2.3. Characterization

FTIR transmittance spectra of the biosorbents were recorded in the region of 4000–400 cm<sup>-1</sup> by using a Scottech-sp-1 spectrophotometer. The surface acidity and basicity of the biosorbents were determined by the Boehm method [37]. About 0.1 g of each sample was mixed with 50 mL of 0.01 M aqueous reactant solution (NaOH, Na<sub>2</sub>CO<sub>3</sub>, NaHCO<sub>3</sub> or HCl). The mixtures were stirred at 500 rpm for 24 h at room temperature. Then, the suspensions were filtrated by a 0.45 µm membrane filter. To determine the oxygenated groups content, back titrations of the filtrate (10 mL) were achieved with HCl (0.01M) solution. Basic groups contents were also determined by back titration of the filtrate with NaOH (0.01 M) solution. The elemental analysis was performed using a CHNS/O analyzer type Flash 2000 EA 1112 (Thermo Fisher Scientific). Before the analysis, the samples were dried overnight at 105°C and cooled in a desiccator. Oxygen content was obtained by the difference between the total percentage (100 wt. %) and the sum of percentages (wt. % dry ash free) of nitrogen, carbon, hydrogen and sulfur. The morphological characteristics were analyzed by scanning electron microscopy using a FEI Quanta 200 model. Small amount of each sample was finely powdered and mounted directly on to aluminum sample holder using two-sided adhesive carbon model. The point of zero charge (pH<sub>PZC</sub>) was determined by the pH drift method according to the method proposed by Noh and Schwarz [23]. The pH of NaCl aqueous solution (50 ml at

0.01 mol/L) was adjusted to successive initial values in the range of 2–12 by addition of HNO<sub>3</sub> and/or NaOH. Moreover, 0.05 g of each biosorbent was added in the solution and stirred for 6 h. The final pH was measured and plotted. The pH<sub>PZC</sub> was determined at the value for which pH<sub>final</sub> = pH<sub>initial</sub>.

#### 2.4. Biosorption studies

Dyes solutions were prepared by dissolving desired weight of each dye in distilled water and necessary concentrations were obtained by dilution. Biosorption experiments were performed in a series of 50 mL beakers containing the desired weight of each biosorbent and 50 mL of the dye solution at desired concentration. These experiments were carried out at a constant agitation of 500 rpm. Effect of pH was investigated by varying pH of solution from 2.00 to 12.00, biosorbents dosage from 0.5 to 5 g/L, contact time from 5 to 180 min, initial dyes concentration from 20 to 500 mg/L, and temperature from 10 to 50°C. The solution pH was adjusted by adding NaOH (0.1 N) or HNO<sub>3</sub> (0.1 N) and measured by a sensION + PH31 pH meter. The temperature was controlled using a thermostatically controlled incubator. In last of each biosorption experiment, the solid phase was separated from the liquid phase by centrifugation at 3400 rpm for 10 min. The final concentrations were determined at maximum absorption wavelength of each dye (Table 1) using a TOMOS V-1100 UV-vis spectrophotometer.

Dyes biosorption capacity and biosorbed yield were calculated by using the following equations:

$$q = \frac{(C_0 - C)}{R} \quad (1)$$

$$\% \text{ Removal} = \frac{(C_0 - C)}{C_0} * 100 \quad (2)$$

where  $q$  (mg/g) is the biosorbed quantity (mg/g),  $C_0$  is the initial dye concentration (mg/L),  $C$  (mg/L) is the dye concentration at a time  $t$  (mg/L), and  $R$  is the mass biosorbents per liter of solution (g/l).

Kinetic and equilibrium parameters were estimated via the non-linear regression using Origin 6.0 software.

### 3. Results and discussion

#### 3.1. Boehm titration of the biosorbents

Boehm titration [38] is one of the most widely methods used to quantify and differentiate surface groups on biosorbents of different acidic or basic groups. The aims of this study were to quantify the functional groups present on cell wall of the Raw-carb, HCl-carb and NaOH-carb. The obtained result was presented in Table 2. From this table it can be seen that the Raw-carb, HCl-carb and NaOH-carb surfaces are constituted mainly of acidic groups which are due to presence of carboxylic, phenolic and lactonic groups and a less quantity of basic groups. It can be noted that the Raw-carb, HCl-carb and NaOH-carb surfaces are composed essentially of acidic groups which are due to presence of carboxylic, phenolic and

Table 2

Chemical groups on the surface of the biosorbents

Biosorbent	Raw-carb	HCl-carb	NaOH-carb
Carboxylic groups (meq/g)	0.4039	0.4000	0.4556
Lactonic groups (meq/g)	0.4500	0.4445	0.4131
Phenolic groups (meq/g)	0.3900	0.3700	0.4066
Total acid groups (meq/g)	1.2439	1.2145	1.2753
Total basic groups (meq/g)	0.4010	0.3900	0.4010

Table 3

Elemental analysis of Raw-carb, HCl-carb and NaOH-carb

Biosorbents	Percentage (%)				
	C	H	N	S	O
Raw-carb	44.02	5.95	0.85	0.00	47.35
HCl-carb	48.03	5.18	1.15	0.00	38.04
NaOH-carb	44.72	6.15	1.06	0.00	45.47

lactonic groups and a less quantity of basic groups. The biosorbents with greater acidic groups will have higher cation exchange properties. According to the experimental data, the NaOH-carb had an important amount of acidic groups than Raw-Carb following by HCl-carb. It was observed that the concentration of carboxylic and phenolic groups in NaOH-carb is higher than those of lactonic groups. The increase of these groups can be due to the rise of the amount of hydrogen and carbon on material after NaOH treatment, see elemental analysis. The quantity of these groups may be demonstrating the order of sorption performance of this studding biosorbents of cadmium and cobalt ions sorption, which are NaOH-carb, Raw-carb and HCl-carb.

#### 3.2. Elemental analysis

Elemental analysis results of Raw-carb, HCl-carb and NaOH-carb are illustrated in Table 3. From the table, it might be seen that the shell carb untreated has greater oxygen content followed by carbon, hydrogen and nitrogen. But after the treatment by HCl, it seems an increase in the carbon and nitrogen content but, it was a reduction in oxygen rate and decreasing of hydrogen. For the material treating by NaOH, we can be seen an increase in the percentage of carbon, hydrogen and nitrogen. Whereas, the amount of oxygen decreased. These results match the Boehm titration which indicates a greater number of carboxylic and phenol groups in NaOH-carb and lactonic groups in HCl-carb. Nevertheless, these biosorbents do not contain the sulfur element. In fact, the treatment by HCl of carob shell decreases the oxygen and hydrogen groups. While, the treatment by NaOH increases the hydrogenated groups.

#### 3.3. FT-IR analysis of the biosorbents

The infrared spectra of Raw-carb, HCl-carb and NaOH-carb are illustrated in Fig. 1. The spectra of Raw-carb has a broad biosorption peaks at around 3200–3600 cm<sup>-1</sup> may be due to the vibration stretching of the O–H bond and

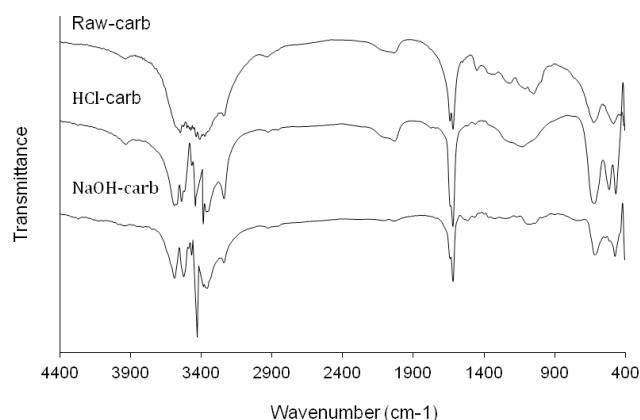


Fig. 1. FT-IR spectra of Raw-carb, HCl-carb and NaOH-carb biosorbents.

suggests the presence of the hydroxyl ( $\text{OH}^-$ ) groups in the cellulose, lignin and water [39]. After the chemical pretreatments, this band was separated into more resolute three bands, two bands at around  $3400$  and  $3300\text{ cm}^{-1}$  are ascribable to vibrations of hydroxyl groups, whereas the position of the band for non-bonded alcohols, phenols and carboxylic acids is usually around  $3500\text{ cm}^{-1}$ . The bands at  $2935\text{ cm}^{-1}$  is due to the C–H stretching vibration. The stretching vibration band at  $2880\text{ cm}^{-1}$  is due to methoxy group ( $\text{CH}_3\text{-O}$ ). The band at  $1618\text{ cm}^{-1}$  is attributed to asymmetric stretching of the carboxylic C=O double band. These bands become finer in the HCl-carb and NaOH-carb. Then, the band at  $1456\text{ cm}^{-1}$  is due to the skeletal C=C vibrations in aromatic rings [40]. Or, the band at  $1075\text{ cm}^{-1}$  is assigned to O–H bonds and C–OH stretching of phenolic groups. The band caused by O–H out-of-plane bending vibrations band is located at  $580\text{ cm}^{-1}$  [41].

### 3.4. pH of zero charge

The  $\text{pH}_{\text{pzc}}$  is an important characteristic in biosorption as it indicates the acidity/basicity of the biosorbent and the net surface charge of the biosorbent in solution. The pHs of zero charge ( $\text{pH}_{\text{pzc}}$ ) of the biosorbents were judged to be 5.4, 2.8 and 6.52 respectively for Raw-carb, HCl-carb and NaOH-carb. It could be seen that the Raw-carb has an acidic surface. After the treatment by HCl, we can observe an increase in the acidity of the material at 2.8. Although, after NaOH treatment, it's appears an increase in the  $\text{pH}_{\text{pzc}}$ . These  $\text{pH}_{\text{pzc}}$  values indicate that the biosorbents acquire a positive charge below a pH of 5.4, 2.8 and 6.52 respectively for Raw-carb, HCl-carb and NaOH-carb. Above these values, the biosorbent surface become negatively charged [42]. Thus, the ionic biosorbent–adsorbate interaction with cationic dyes (MB and MG) becomes progressively significant for pH higher than 5.4, 2.8 and 6.52. These  $\text{pH}_{\text{pzc}}$  values are in agreement with Boehm titration result, which show a dominance of acidic groups at the surface of the biosorbents.

### 3.5. Morphology of the biosorbents

The scanning electron microphotographs (SEM) of Raw-carb, HCl-carb and NaOH-carb are represented in

Fig. 2. It is clear from this images that there is a big difference between the surface morphology of the raw and the chemically treated carb shell. We can see from this figure, there was no poreus surface texture of Raw-carb. However, the surface morphology of the treating carb shell by HCl represents the appearance of new pores due to the reaction between the composition of raw material and the activating agent. Also, the figure shows clearly that the surface of NaOH-carb was rough and contained pores of various sizes and shapes. Based on this result we can conclude that the NaOH is a strong agent effective in creating well-developed pores on the surface of the carb shell. Hence, the highly porosity of NaOH-carb could explain the large sorption capacity of the both studied dyes.

### 3.6. Effect of pH on the biosorption

The pH of aqueous solution is one of the most important factors in the biosorption of cationic dyes. It has an impact on both the surface binding-sites of the biosorbent and the ionization process of the dye molecule [43]. Fig. 3 depicts the effect of pH on biosorption of MB and MG onto Raw-carb, HCl-carb and NaOH-carb. It is clear from this figure that the biosorption capacity increased when the solution pH increased. This result may be due to change in surface charge of both the dyes molecules and functional groups of biosorbents. Also, lower biosorption of MB and MG at acidic pH is due to the presence of excess  $\text{H}^+$  ions competing with dye cations for the sorption sites [44]. However, at higher pH values, more negatively charged surface sites are available, which facilitates the biosorption of dye cations. The  $\text{pH}_{\text{pzc}}$  were 5.4 for Raw-carb, 2.8 for HCl-carb and 6.52 for NaOH-carb. These  $\text{pH}_{\text{pzc}}$  values indicate that the biosorbents acquire a positive charge below pH of 5.4, 2.8 and 6.52, respectively, for Raw-carb, HCl-carb and NaOH-carb. While, above these values, the biosorbent surface become negatively charged [42] which increase the sorption performance of these biosorbents.

### 3.7. Effect of biosorbents dosage

The effect of biosorbent dosage on the biosorption of MB and MG on the three biosorbents is presented in Fig. 4. The figure shows that the increase in biosorbent dosage leads in a sharply increase of the biosorption yield. For MB, the biosorption yield increased from 18.12 to 79.26%, from 20.94 to 77.64% and from 46.84 to 99.04%, when the biosorbents dosage was increased from 0.25 to 2 g/L, respectively for Raw-carb, HCl-carb and NaOH-carb. For MG, the biosorption yield increased from 36.27 to 84.23%, from 40.59 to 81.31% and from 54.60 to 97.31 %, when the biosorbents dosage was increased from 0.25 to 3 g/L, respectively for Raw-carb, HCl-carb and NaOH-carb. This result has been due to the availability of the biosorption sites with the increasing of the biosorbent dosage [45]. Moreover, there is an increase in biosorbent dosage over 2 g/L for MB and 4 g/L for MG. This could be explained by the decrease in force of the mass transfer at low concentration of dyes in solution. According to the figure, the NaOH-carb was presented a strongly potential of fixing MB and MG.



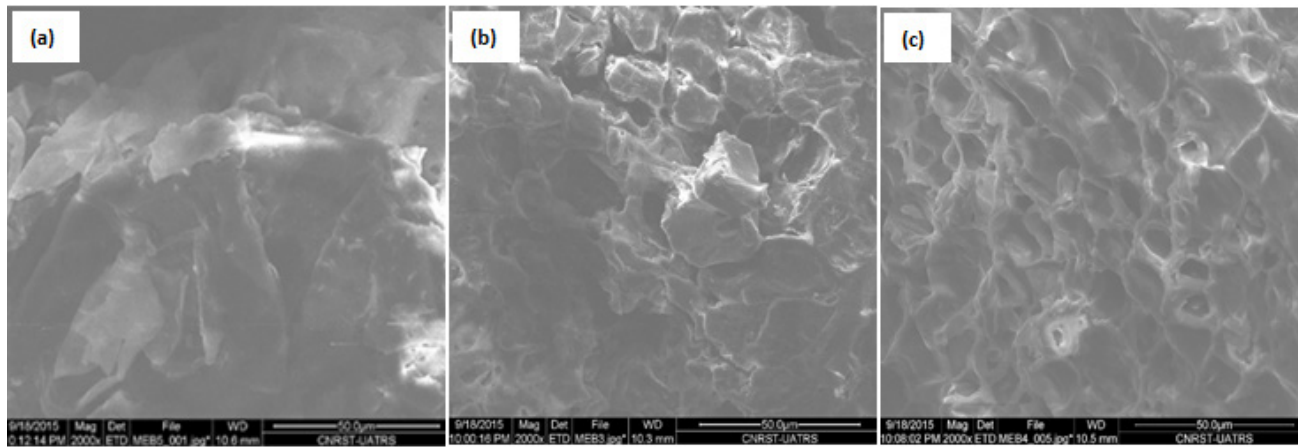


Fig. 2. SEM images of: (a) Raw-carb, (b) HCl-carb and (c) NaOH-carb biosorbents.

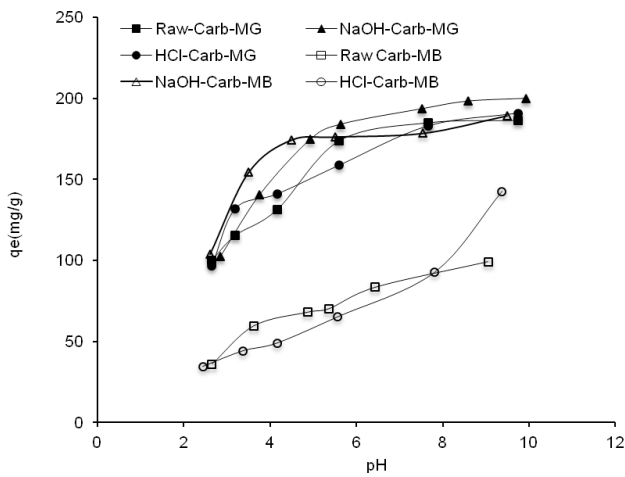


Fig. 3. Effect of pH on the biosorption of MB and MG onto biosorbents: C<sub>0</sub> = 100 mg/L, contact time = 120 min, R = 0.5 g/L, and T = 25°C.

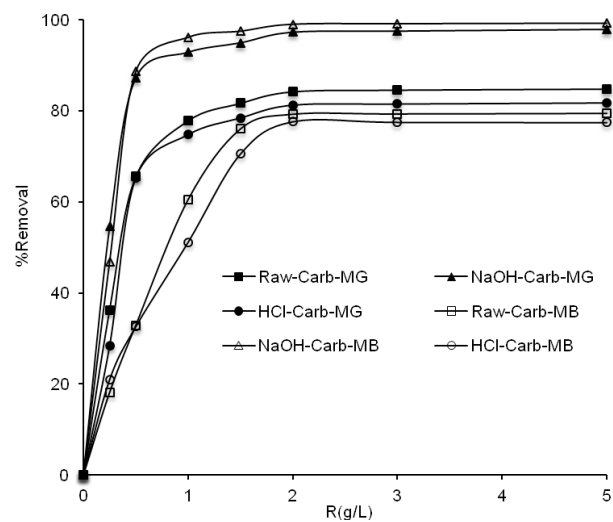


Fig. 4. Effect of biosorbents dosage of the removal of MB and MG: C<sub>0</sub> = 100 mg/L, contact time = 120 min, initial pH, and T = 25°C.

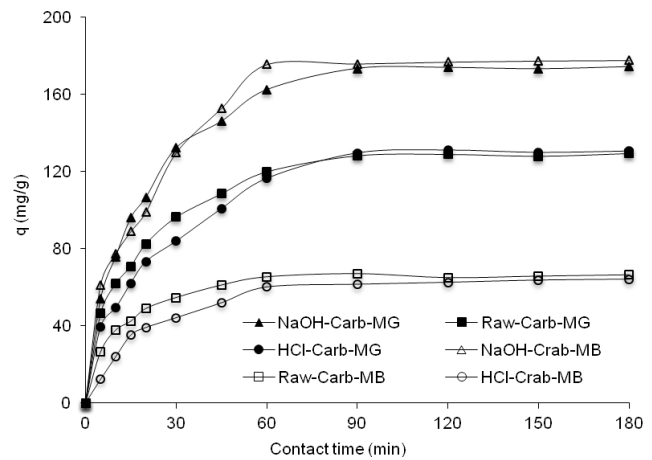


Fig. 5. Kinetics of MB and MG biosorption onto biosorbents: C<sub>0</sub> = 100 mg/L, R = 0.5 g/L, initial pH, temperature = 25°C.

### 3.8. Biosorption kinetics

The contact time is an important parameter in all transfer phenomena such as biosorption. Fig. 5 shows the plot of MB and MG biosorption versus contact time. It is clear from this figure that the amount of MB and MG adsorbed increases with increasing contact time at an equilibrium time. In fact, the biosorption was rapid during the first of the process and then gradually decreased to become constant after the equilibrium point. The rapid biosorption of MB and MG during the initial stages may result from the availability of the uncovered surface and active sites on the biosorbent surface. The equilibrium time was reached at 60 min for MB and at 90 min for MG. To evaluate the kinetics involved in the process of biosorption, pseudo-first-order and pseudo-second-order rate equations were applied based on the regression coefficient (*r*<sup>2</sup>) and the amount of dye biosorbed per unit weight of the biosorbent.

The first-order rate expression of Lagergren based on solid capacity is generally expressed as follows [46]:

$$q = q_e(1 - e^{-k_1 t}) \tag{3}$$

where  $q_e$  and  $q$  (both in mg/g) are, respectively, the amounts of dye biosorbed at equilibrium and at any time  $t$  (min) and  $k_1$  (1/min) is the rate constant of biosorption.

The pseudo-second-order model is derived on the basis of the sorption capacity of the solid phase. This kinetic model was expressed as:

$$q = \frac{k_2 q_e^2 t}{1 + k_2 q_e t} \tag{4}$$

where  $k_2$  (g/mg min) is the rate constant of pseudo-second-order biosorption.

Parameters of the pseudo-first-order and pseudo-second-order kinetic models were estimated with the aid of the non linear regression. The obtained results and the correlation coefficients,  $r^2$ , are given in Table 4. This result indicated that the pseudo-first-order model had values of sorption capacities close to those experimental ( $Q_{exp}$ ). Hence, these calculated values are well agreed with the experimental data. Therefore, pseudo-first-order kinetic model provided a best description for the biosorption of MB and MG onto all three biosorbents. This can be explained by the speed rapidity of the transfer molecules MB and MG to the surface of the biosorbent.

### 3.9. Biosorption isotherms

To better understand the distribution process of adsorbate molecules between the liquid and solid phases, the biosorption isotherm has been investigated [47]. Fig. 6. presents the biosorption isotherms of MG and MB onto Raw-carb, HCl-carb and NaOH-carb. The figure shows that the equilibrium biosorption capacities of the three biosorbents increased with a rise in dye initial concentration. This increase may be due to the high driving force for mass transfer. According to the Giles classification, the isotherms of the both dyes onto Raw-carb, HCl-carb and NaOH-carb were presented in the form of the type L [48]. In the current study, isotherm models were adopted to analyze the experimental equilibrium data are Langmuir, Freundlich, Temkin, and Dubinin–Radushkevich models.

#### 3.9.1. Langmuir model

This model assumes monolayer coverage of biosorbent and biosorption occurs over specific homogenous sites on

the biosorbent [49]. The Langmuir isotherm is given by the following equation:

$$q_e = \frac{q_m K_L C_e}{1 + K_L C_e} \tag{5}$$

where  $q_m$  (mg/g) is the maximum monolayer biosorption capacity,  $K_L$  (L/mg) is the Langmuir equilibrium constant related to the biosorption affinity and  $C_e$  is the equilibrium concentration.

#### 3.9.2. Freundlich model

It is an empirical equation which indicates that the biosorption process takes place on a heterogeneous surface and biosorption capacity is related to the concentration of dye at equilibrium [50].

The form of the Freundlich equation is given by the following expression:

$$q_e = K_f C_e^{1/n} \tag{6}$$

where  $K_f$  ( $\text{mg}^{1-1/n}/\text{g}/\text{L}^n$ ) is the Freundlich constant and  $n$  is the heterogeneity factor. The  $K_f$  value is related to the biosorption capacity; while  $1/n$  value is related to the biosorption intensity.

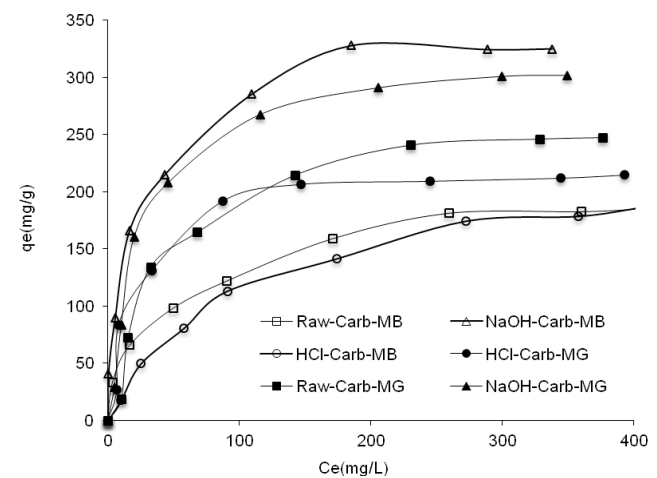


Fig. 6. Biosorption isotherms of MB and MG onto biosorbents:  $R = 0.5 \text{ g/L}$ , initial pH, contact time = 120 min, temperature = 25°.

Table 4  
Pseudo-first-order and pseudo-second-order kinetic parameters for the biosorption of MB and MG

Dyes	Biosorbents	$q_e$ (mg/g)	Pseudo first-order			Pseudo second-order		
			$q_e$ (mg/g)	$k_1$ (1/min)	$r^2$	$q_e$ (mg/g)	$k_2$ (g/mgmin)	$r^2$
MB	Raw-carb	65.329	65.607	0.078	0.988	71.056	0.001	0.993
	HCl-carb	60.103	62.773	0.046	0.993	72.538	0.001	0.992
	NaOH-carb	175.484	176.270	0.052	0.981	193.724	0.001	0.990
MG	Raw-carb	128.197	126.836	0.053	0.978	140.310	0.001	0.993
	HCl-carb	129.609	129.321	0.041	0.979	149.622	0.001	0.988
	NaOH-carb	173.349	171.486	0.052	0.988	194.261	0.001	0.995

### 3.9.3. Temkin model

The Temkin isotherm model assumes that the heat of adsorption of all the molecules in the layer decreases linearly with coverage due to adsorbent–adsorbate interactions. The biosorption is characterized by uniform distribution of the binding energies [51]. The Temkin isotherm can be written in the following form:

$$q_e = B \ln (K_T C_e) \quad (7)$$

where  $B = RT/b$   $T$  (K) is the absolute temperature and  $R$  is the universal gas constant (8.314 J/mol).  $B$  is the Temkin constant related to the heat of adsorption (kJ/mol) and  $K_T$  is the empirical Temkin constant related to the equilibrium binding constant related to the maximum binding energy (L/mg).

### 3.9.4. Dubinin radushkevich model

Dubinin radushkevich isotherm is generally applied to express the adsorption mechanism with a Gaussian energy distribution onto a heterogeneous surface [52]. The Dubinin radushkevich isotherm has been expressed as:

$$q_e = q_m \exp(-B\epsilon^2) \quad (8)$$

$$\epsilon^2 = RT \ln\left(1 + \frac{1}{C_e}\right) \quad (9)$$

where  $B$  is a constant related to the adsorption energy,  $q_m$  is the theoretical saturation capacity, and  $\epsilon$  is the Polanyi potential.

### 3.9.5. Analysis of biosorption isotherms

The calculated isotherm parameters for each model were determined by non linear regression analysis. The obtained values are illustrated in Table 5. This table indicates that the Langmuir model has high correlation coefficients ( $r^2 > 0.997$ ) for the both dyes biosorption onto the three biosorbents. This result suggests that the Langmuir model present a best fitting of experimental equilibrium data. Therefore, based on the Langmuir assumptions, it seems that the MB and MG were adsorbed on monolayer with a homogeneously distributed of binding sites on the biosorbent surface. It

was then no interaction or competitive interaction between biosorbed molecules. The maximum Langmuir monolayer biosorption capacities were 217.15, 232.44 and 342.21 mg/g for MB and 233.40, 291.74 and 327.89 mg/g in the case of MG, respectively, for Raw-carb, HCl-carb and NaOH-carb.

On the other hand, it could be seen that the biosorption capacities of NaOH-carb is specifically greater than those of Raw-carb and HCl-carb. This might be due to the increase in carbon and hydrogen quantities and carboxylic groups that are estimated by the elemental analysis and Bohem titration. Also, the morphology of NaOH-carb presents pores well developed, which indicate a highly adsorptive efficiency of the material treated by NaOH.

For the Freundlich model, the correlation coefficients are lower. This model did not provide a more description about the saturation biosorption capacity such as the Langmuir model. Whereas, the values of  $n > 1$  indicates a favorable biosorption under experimental conditions for MB and MG by the three biosorbents. The Temkin model provides a calculation about equilibrium binding constant corresponding to the maximum binding energy,  $K_T$ . This model presents a correlation coefficient in order of  $r^2 < 0.989$  for the both dyes. Further, the Dubinin–Radushkevich model has low values  $q_m$ . The comparison of the optimization data of the four isotherm models, it was concluded that the Langmuir model is the most appropriate to fit the biosorption isotherms. Although, the Temkin model is more adapted than Freundlich and Dubinin–Radushkevich models.

For more confirmed the high potential efficiencies of Raw-carb, HCl-carb and NaOH-carb to adsorb the basic dyes, a comparison of biosorption capacities obtained in this study with those of some biosorbents that reported in literature, was investigated. Table 6 exhibits the d maximum biosorption capacities of these biosorbents. From this table, it may be seen that Raw-carb, HCl-carb and NaOH-carb present a higher sorption capacities compared to those in the literature. This result can be due to the nature of functional groups present in Raw-carb, HCl-carb and NaOH-carb that are engaged in binding interaction biosorbent-adsorbant.

### 3.10. Effect of temperature

The effect of temperature on the biosorption of dyes is very important in the real application of biosorption as various textile and other dyes effluent produced at relatively different temperatures. Fig. 6. reports the variation

Table 5  
Models isotherm parameters for the biosorption of MB and MG onto biosorbents

Dye	Adsorbent	Langmuir			Freundlich			Temkin			Dubinin–Radushkevich		
		$q_m$	$K_L$	$r^2$	$K_F$	$n$	$r^2$	$K_T$	$B$	$r^2$	$q_m$	$B$	$r^2$
MB	Raw-carb	217.15	0.016	0.996	33.66	3.44	0.987	0.20	56.72	0.972	179.25	0.074	0.875
	HCl-carb	232.45	0.010	0.997	19.21	2.61	0.990	0.12	52.35	0.990	175.98	0.011	0.881
	NaOH-carb	342.21	0.061	0.988	73.65	3.72	0.975	0.38	54.21	0.944	316.28	0.067	0.884
MG	Raw-carb	233.40	0.032	0.950	32.88	3.09	0.949	0.35	54.57	0.973	213.11	0.223	0.972
	HCl-carb	291.74	0.017	0.978	26.69	2.65	0.937	0.17	39.74	0.979	227.57	0.128	0.939
	NaOH-carb	327.90	0.038	0.992	53.01	3.21	0.930	0.42	38.51	0.972	278.91	0.075	0.938

Table 6  
Comparison of biosorption capacity ( $q_m$ ) of Raw-carb, HCl-carb and NaOH-carb for MB and MG with different biosorbents

Biosorbent	MB $q$ (mg/g)	MG $q$ (mg/g)	Refs
D. harra	185.59	64.37	[36]
G. coronaria L	258.76	117.32	[36]
Natural zeolite	19.94	–	[53]
Sugar extracted rice	8.13	–	[24]
Luffa cylindrica	49.46	–	[54]
Aspergillus fumigatus	125	–	[55]
Fly ash	5.718	–	[56]
Saw dust	32.26	–	[57]
Raw clay	27.49	–	[58]
Calcined clay	13.44	–	[58]
Brazil nut shells	7.81	–	[59]
Clayey soil	–	78.57	[60]
EM based compost	–	150,8	[61]
Walnut shell	–	90.8	[62]
Aerobic granules	–	56.8	[63]
Beech sawdust	–	83.21	[64]
Pleurotusostreatus	–	32.33	[65]
Groundnut husk unmodified	–	44.84	[66]
Raw-carb	217.15	233.40	This study
HCl-carb	232.44	291.74	This study
NaOH-carb	342.21	327.89	This study

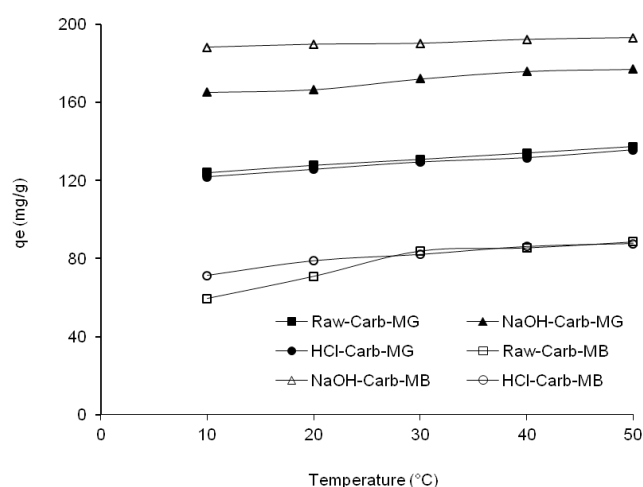


Fig. 7. Effect of temperature on MB and MG biosorption onto biosorbents:  $R = 0.5$  g/L, initial pH, contact time = 120 min,  $C_0 = 100$  mg/L.

in biosorbed quantities of MB and MG onto Raw-carb, HCl-carb and NaOH-carb as function of solution temperature. According to the obtained data, it was observed that the increase in temperature promotes a small increasing of the biosorbed amount of MB and MG. This indicated that the increase in temperature does not have significant influence on the biosorption of MB and MG onto the three biosor-

bents. Increasing the temperature is considered as an effect to increase the rate of diffusion of the adsorbate molecules across the external boundary layer and in the internal pores of the adsorbent particle, owing to the decrease in the viscosity of the solution [67].

#### 4. Conclusion

During this work, raw carb shell and chemically treated carb shell were used as low-cost natural biosorbents for studying the elimination of MB and MG from aqueous solutions. The ability of these biosorbents was investigated using various experiments. Bases on these studies, the best biosorption was obtained at basic pH medium. The biosorption yield increases with increasing biosorbent dosage with an optimum at 0.5 g/L. The sorption process was very rapid, the equilibrium time was obtained at 60 min for MB and 90 min for MG. The best kinetic model was the pseudo-first-order. The biosorption equilibrium data were well correlated to the Langmuir isotherm model under these optimum conditions. The temperature does not have much influence on the biosorption performance. Lastly, it can be concluded that the chemical pretreatment of the raw carob shell by NaOH mad an efficient biosorbent of MB and MG from aqueous solutions.

#### References

- [1] K.H. Gonawala, M.J. Mehta, Removal of color from different dye wastewater by using ferric oxide as an adsorbent, *Int. J. Eng. Res. Appl.*, 4 (2014) 102–109.
- [2] M. Joshi, R. Bansal, R. Purwar, Colour removal from textile effluents, *Indian J. Fibre Text. Res.*, 29 (2004) 239–259.
- [3] S. Banerjee, M.C. Chattopadhyaya, Adsorption characteristics for the removal of a toxic dye, tartrazine from aqueous solutions by a low cost agricultural by-product, *Arabian J. Chem.*, 10 (2017) S1629–S1638.
- [4] A. Mittal, Retrospection of Bhopal gas tragedy, *Toxicol. Environ. Chem.*, 98 (2016) 1079–1083.
- [5] K. Kapadia, F. Cheung, W. Lee, R. Thalappillil, F. Barry Florence, J. Kim, Methylene blue causing serotonin syndrome following cystocele repair, *Urol. Case Rep.*, 9 (2016) 15–17.
- [6] R. Gopinathan, J. Kanhere, J. Banerjee, Effect of malachite green toxicity on non target soil organisms, *Chemosphere*, 120 (2015) 637–644.
- [7] F. Ding, X.N. Li, J.X. Diao, Y. Sun, L. Zhang, L. Ma, X.L. Yang, L. Zhang, Y. Sun, Potential toxicity and affinity of triphenylmethane dye malachite green to lysozyme, *Ecotoxicol. Environ. Saf.*, 78 (2012) 41–49.
- [8] G. Sudarjanto, B. Keller-Lehmann, J. Keller, Optimization of integrated chemical-biological degradation of a reactive azo dye using response surface methodology, *J. Hazard. Mater.*, 138 (2006) 160–168.
- [9] A. Abaamrane, S. Qourzal, N. Barka, S. Mañour-Billah, A. Assabbane, Y. Ait-Ichou, Optimal decolorization efficiency of indigo carmine by  $TiO_2$ /UV photocatalytic process coupled with response surface methodology, *Orient. J. Chem.*, 28(3) (2012) 1091–1098.
- [10] F. Harrelkas, A. Azizi, A. Yaacoubi, A. Benhammou, M.N. Pons, Treatment of textile dye effluents using coagulation-flocculation coupled with membrane processes or adsorption on powdered activated carbon, *Desalination*, 235 (2009) 330–339.
- [11] C. Berberidou, S. Avlonitis, I. Poullos, Dyestuff effluent treatment by integrated sequential photocatalytic oxidation and membrane filtration, *Desalination*, 249 (2009) 1099–1106.



- [12] M.H.P. Santana, L.M.D. Silva, A.C. Freitas, J.F.C. Boodts, K.C. Fernandes, L.A. De Faria, Application of electrochemically generated ozone to the discoloration and degradation of solutions containing the dye Reactive Orange 122, *J. Hazard. Mater.*, 164 (2009) 10–17.
- [13] C.A. Basha, N.S. Bhadrinarayana, N. Anantharaman, K.M. Meera Sheriffa Begum, Heavy metal removal from copper smelting effluent using electrochemical cylindrical flow reactor, *J. Hazard. Mater.*, 152 (2008) 71–78.
- [14] N. Daneshvar, H.A. Sorkhabi, M.B. Kasiri, Decolorization of dye solution containing Acid Red 14 by electro coagulation with a comparative investigation of different electrode connections, *J. Hazard. Mater.*, B 112 (1–2) (2004) 55–62.
- [15] M. Bayramoglu, M. Kobya, O.T. Can, M. Sozbir, Operating cost analysis of electro coagulation of textile dye wastewater, *Sep. Purif. Technol.*, 37 (2004) 117–125.
- [16] R. Elmoubarki, F.Z. Mahjoubi, A. Elhalil, H. Tounsadi, M. Abdennouri, M. Sadiq, S. Qourzal, A. Zouhri, N. Barka, Ni/Fe and Mg/Fe layered double hydroxides and their calcined derivatives: preparation, characterization and application on textile dyes removal, *J. Mater. Res. Technol.*, 6(3) (2017) 271–283.
- [17] H. Feather, A remarkable adsorbent for dye removal, J. Mittal, A. Mittal, in S.K. Sharma, ed., *Green Chemistry for Dyes Removal from Wastewater*, chap. 11, Scrivener Publishing LLC, USA, 2015, pp. 409–457.
- [18] A. Mittal, R. Ahmed, I. Hassan, Iron oxide-impregnated dextrin nano composite: synthesis and its application for the biosorption of Cr (VI) ions from aqueous solution, *Desal. Water Treat.*, 57 (2016) 15133–15145.
- [19] A. Mittal, R. Ahmed, I. Hassan, Biosorption of Pb<sup>2+</sup>, Ni<sup>2+</sup> and Cu<sup>2+</sup> ions from aqueous solutions by L-cystein-modified montmorillonite-immobilized alginate nano composite, *Desal. Water Treat.*, 57 (2016) 17790–17807.
- [20] A. Mittal, R. Ahmed, I. Hassan, Poly (methyl methacrylate)-grafted alginate/Fe<sub>3</sub>O<sub>4</sub> nano composite: synthesis and its application for the removal of heavy metal ions, *Desal. Water Treat.*, 57 (2016) 19820–19833.
- [21] R. Abdallah, S. Taha, Biosorption of methylene blue from aqueous solution by nonviable *Aspergillus fumigatus*, *Chem. Eng. J.*, 195–196 (2012) 69–76.
- [22] M. Asgher, H.N. Bhatti, Mechanistic and kinetic evaluation of biosorption of reactive azo dyes by free, immobilized and chemically treated *Citrus sinensis* waste biomass, *Ecol. Eng.*, 36 (2010) 1660–1665.
- [23] R. Hazzaa, M. Hussein, Adsorption of cationic dye from aqueous solution onto activated carbon prepared from olive stones, *Environ. Technol. Innov.*, 4 (2015) 36–51.
- [24] M.S.U. Rehman, I. Kim, J.I. Han, Adsorption of methylene blue dye from aqueous solution by sugar extracted spent rice biomass, *Carbohydr. Polym.*, 90 (2012) 1314–1322.
- [25] A. Aziz, M.S. Ouali, E.H. Elandaloussi, L.C.D. Menorval, M. Lindheimer, Chemically modified olive stone: A low-cost sorbent for heavy metals and basic dyes removal from aqueous solutions, *J. Hazard. Mater.*, 163 (2009) 441–447.
- [26] H. Deng, J. Lu, G. Li, G. Zhang, X. Wang, Adsorption of methylene blue on adsorbent materials produced from cotton stalk, *Chem. Eng. J.*, 172 (2011) 326–334.
- [27] A. Machrouhi, A. Elhalil, M. Farnane, F.Z. Mahjoubi, H. Tounsadi, M. Sadiq, M. Abdennouri, N. Barka, Adsorption behavior of methylene blue onto powdered *Ziziphus lotus* fruit peels and avocado kernels seeds, *J. Appl. Surf. Interface.*, 1 (1–3) (2017) 49–56.
- [28] M.P. Elizalde-González, W. Geyer, M.R.G. Guevara-Villa, J. Mattusch, A.A. Pelaez-Cid, R. Wennrich, Characterization of an adsorbent prepared from maize waste and adsorption of three classes of textile dyes, *Colloids Surf A-physicochemical, Eng. Asp.*, 278 (2006) 89–97.
- [29] M.M. Davila-Jiménez, M.P. Elizalde-Gonzalez, V. Hernandez-Montoya, Performance of mango seed adsorbents in the adsorption of anthraquinone and azo acid dyes in single and binary aqueous solutions, *Bioresour. Technol.*, 100 (2009) 6199–6206.
- [30] B. Zhao, W. Xiao, Y. Shang, H. Zhu, R. Han, Adsorption of light green anionic dye using cationic surfactant-modified peanut husk in batch mode, *Arabian J. Chem.*, 10 (2017) S3595–S3602.
- [31] A.A. Peláez-Cid, I. Velázquez-Ugalde, A.M. Herrera-González, J. García-Serrano, Textile dyes removal from aqueous solution using *Opuntia ficus-indica* fruit waste as adsorbent and its characterization, *J. Environ. Manage.*, 130 (2013) 90–97.
- [32] V. Ponnusami, S.N. Srivastava, Studies on application of teak leaf powders for the removal of color from synthetic and industrial effluents, *J. Hazard. Mater.*, 169 (2009) 1159–1162.
- [33] A. Mittal, D. Kaur, A. Malviya, J. Mittal, V.K. Gupta, Adsorption studies on the removal of coloring agent phenol red from wastewater using waste materials as adsorbents. *J. Colloid. Interface Sci.*, 337 (2009) 345–354.
- [34] A. Mittal, L. Kurup, column operations for the removal and recovery of a hazardous dye 'acid red - 27' from aqueous solutions, using waste materials - bottom ash and de-oiled soya, *Ecol. Environ. Conserv.*, 13 (2006) 181–186.
- [35] M. Mahadeva Swamy, B.M. Nagabhushanac, R. Hari Krishnac, Nagaraju Kottamc, R.S. Raveendrad, P.A. Prashanth, Fast adsorptive removal of methylene blue dye from aqueous solution onto a wild carrot flower activated carbon: isotherms and kinetics studies, *Desal. Water Treat.*, 57 (2016) 21863–21869.
- [36] H. Tounsadi, A. Khalidi, M. Abdennouri, N. Barka, Potential capability of natural biosorbents: *Diplotaxis harra* and *Glebionis coronaria* L. on the removal efficiency of dyes from aqueous solutions, *Desal. Water Treat.*, 57 (2015) 16633–16642.
- [37] H.P. Boehm, E. Diehl, W. Heck, R. Sappok, Surface oxides of carbon, *Angew. Chem. Internat. Ed.*, 3 (1964) 669–677.
- [38] J.S. Noh, J.A. Schwarz, Estimation of the point of zero charge of simple oxides by mass titration, *J. Colloid. Interface Sci.*, 130 (1989) 157–164.
- [39] F. Rubio, J.A.C. Gonçalves, A.P. Meneghel, C.R.T. Tarley, D. Schwantes, G.F. Coelho, Removal of cadmium from water using by-product *Crambe abyssinica* Hochst seeds as biosorbent material, *Water Sci. Technol.*, 68 (2013) 227–233.
- [40] J.C.P. Vaghetti, E.C. Lima, B. Royer, B.M. Da Cunha, N.F. Cardoso, J.L. Brasil, S.L.P. Dias, Pecan nutshell as biosorbent to remove Cu(II), Mn(II) and Pb(II) from aqueous solutions, *J. Hazard. Mater.*, 162 (2009) 270–280.
- [41] J. Yang, K. Qiu, Preparation of activated carbon from walnut shells via vacuum chemical activated and their application for methylene blue removal, *Chem. Eng. J.*, 165 (2010) 209–217.
- [42] I. Bakas, K. Elatmani, S. Qourzal, N. Barka, A. Assabbane, I. Aït-Ichou, A comparative adsorption for the removal of p-cresol from aqueous solution onto granular activated charcoal and granular activated alumina, *J. Mater. Environ. Sci.*, 5 (2014) 675–682.
- [43] X.S. Wang, Y. Zhou, J. Yu, C. Sun, The removal of basic dyes from aqueous solutions using agricultural by-products, *J. Hazard. Mater.*, 157 (2008) 374–385.
- [44] O. Hamdaoui, Batch study of liquid-phase adsorption of methylene blue using cedar sawdust and crushed brick, *J. Hazard. Mater.*, 135 (2006) 264–273.
- [45] L. Wang, J. Zhang, R. Zhao, C. Li, Y. Li, C. Zhang, Adsorption of basic dyes on activated carbon prepared from *Polygonum orientale* Linn: equilibrium, kinetic and thermodynamic studies, *Desalination*, 254 (2010) 68–74.
- [46] S. Lagergren, About the theory of so-called adsorption of soluble substance Seven *Vetenskapsakad. HandBand*, 24 (1898) 1–39.
- [47] P. Senthil Kumar, K. Ramakrishnan, S.D. Kiruphaand, S. Sivanesan, Thermodynamic and kinetic studies of cadmium adsorption from aqueous solution onto rice husk, *Braz. J. Chem. Eng.*, 27 (2010) 347–355.
- [48] C.H. Giles, D. Smith, A. Huitson, A general treatment and classification of the solute adsorption isotherm, *J. Colloid. Interface Sci.*, 47 (1974) 755–765.
- [49] I. Langmuir, The constitution and fundamental properties of solids and liquids, *J. Am. Chem. Soc.*, 38 (1916) 2221–2295.
- [50] H. Freundlich, W. Heller, The Adsorption of cis- and trans-azobenzene, *J. Am. Chem. Soc.*, 61 (1939) 2228–2230.

- [51] M.J. Temkin, V. Pyzhev, Kinetics of ammonia synthesis on promoted iron catalysts, *Acta Physicochim. URSS*, 12 (1940) 217–222.
- [52] M.M. Dubinin, L.V. Radushkevich, The equation of the characteristic curve of the activated charcoal, *Proc. Acad. Sci. USSR Phys. Chem. Sec.*, 55 (1947) 331–337.
- [53] R. Han, J. Zhang, P. Han, Y. Wang, Z. Zhao, M. Tang, Study of equilibrium, kinetic and thermodynamic parameters about methylene blue adsorption onto natural zeolite, *Chem. Ing. J.*, 145 (2009) 496–504.
- [54] N. Boudechiche, H. Mokaddem, Z. Sadaoui, M. Trari, Biosorption of cationic dye from aqueous solutions onto lignocellulosic biomass (*Luffa cylindrica*): characterization, equilibrium, kinetic and thermodynamic studies, *Int. J. Ind. Chem.*, 7 (2016) 167–180.
- [55] R. Abdallah, S. Taha, Biosorption of methylene blue from aqueous solution by nonviable *Aspergillus fumigatus*, *Chem. Eng. J.*, 195–196 (2012) 69–76.
- [56] K.V. Kumar, V. Ramamurthi, S. Sivanesan, Modeling the mechanism involved during the sorption of methylene blue onto fly ash, *J. Colloid. Interf. Sci.*, 284 (2005) 14–21.
- [57] D.S. De, J.K. Basu, Adsorption of methylene blue on to a low cost adsorbent developed from saw dust, *Indian J. Environ. Prot.*, 19 (1998) 416–421.
- [58] D. Ghosh, K.G. Bhattacharyya, Removing colour from aqueous medium by sorption on natural clay: a study with methylene blue, *Indian J. Environ. Prot.*, 21 (2001) 903–991.
- [59] S.M.O. Brito, H.M.C. Andrade, L.F. Soares, R.P. De Azevedo, Brazil nut shells as a new biosorbent to remove methylene blue and indigo carmine from aqueous solutions, *J. Hazard. Mater.*, 174 (2010) 84–92.
- [60] P. Saha, S. Chowdhury, S. Gupta, I. Kumar, Insight into adsorption equilibrium, kinetics and thermodynamics of Malachite Green onto clayey soil of Indian origin, *Chem. Eng. J.*, 165 (2010) 874–882.
- [61] T. Bhagavathi Pushpa, J. Vijayaraghavan, S.J. Sardhar Basha, V. Sekaran, K. Vijayaraghavan, J. Jegan, Investigation on removal of malachite green using EM based compost as adsorbent, *Eco-toxicol. Environ. Saf.*, 118 (2015) 177–182.
- [62] M.K. Dahri, M.R.R. Kooh, L.B.L. Lim, Water remediation using low cost adsorbent walnut shell for removal of malachite green: Equilibrium, kinetics, thermodynamic and regeneration studies, *J. Environ. Chem. Eng.*, 2 (2014) 1434–1444.
- [63] X.F. Sun, S.G. Wang, X.W. Liu, W.X. Gong, N. Bao, B.Y. Gao, H.Y. Zhang, Biosorption of Malachite Green from aqueous solutions onto aerobic granules: Kinetic and equilibrium studies, *Biores. Technol.*, 99 (2008) 3475–3483.
- [64] A. Witek-Krowiak, Analysis of influence of process conditions on kinetics of malachite green biosorption onto beech sawdust, *Chem. Eng. J.*, 171 (2011) 976–985.
- [65] Z. Chen, H. Deng, C. Chen, Y. Yang, H. Xu, Biosorption of malachite green from aqueous solutions by *Pleurotus ostreatus* using Taguchi method, *J. Environ. Health Sci. Eng.*, (2014) doi:10.1186/2052-336X-12-63.
- [66] B.J. Titilayo, B. Adesina, N.M. Olubunmi, A.S. Akinyeye, I.A. Ayodeji, Kinetics and thermodynamic studies of adsorption of malachite green onto unmodified and EDTA-modified groundnut husk, *Pure Appl. Chem.*, 6 (2012) 141–152.
- [67] M. Dogan, M. Alkan, O. Demirbas, Y. Ozdemir, C. Ozmetin, Adsorption kinetics of maxilon blue GRL onto sepiolite from aqueous solutions, *Chem. Eng. J.*, 124 (2006) 89–101.